Marine Biology (2003) 143: 995–1011
DOI 10.1007/s00227-003-1129-1

F. Rodríguez · M. Varela · E. Fernández · M. Zapata

Phytoplankton and pigment distributions in an anticyclonic slope water oceanic eddy (SWODDY) in the southern Bay of Biscay

Received: 27 January 2003 / Accepted: 6 May 2003 / Published online: 24 June 2003

Abstract An anticyclonic slope water oceanic eddy (SWODDY), named AE6, was sampled in the southern Bay of Biscay from 12 to 31 August 1998 to assess changes in the abundance and composition of phytoplankton assemblages related to the mesoscale feature. SWODDY AE6 showed characteristic biological signatures. A twofold increase in chlorophyll *a* concentration was found at the eddy centre relative to surrounding waters. Picoplankton cells accounted for a lower fraction of total chlorophyll *a* values at the eddy centre (44–50%) than outside the eddy (54–61%). Microscopic cell counts and HPLC pigment analysis showed that diatoms were almost entirely confined to the eddy centre, but both techniques yielded different results when studying other phytoplankton groups. Microscopic cell counts indicated that the spatial distribution of diatoms, dinoflagellates and unidentified flagellates was significantly influenced by SWODDY AE6, showing maximum abundance inside the mesoscale feature. HPLC pigment analysis provided more detailed information about the composition of pico–nanoplanktonic organisms. Pigment data processed by means of the CHEMTAX program showed "chlorophytes", "haptophytes" and "dinoflagellates II" (having haptophyte-like pigments and gyroxanthin-diester) as the more abundant "pigment classes" at the eddy centre, whereas dominance of "chlorophytes" and higher contribution of "cyanobacteria" (type *Synechococcus*) were estimated in the surrounding waters.

Communicated by S.A. Poulet, Roscoff

F. Rodríguez (✉)
Station Biologique, UPR 9042, Centre Nationale de la Recherche Scientifique et Université Pierre et Marie Curie,
BP 74, 29682 Roscoff Cedex, France
E-mail: rodrigue@sb-roscoff.fr
Tel.: +33-2-98292323
Fax: +33-2-98292324

M. Varela
Instituto Español de Oceanografía,
Centro Costero de A Coruña, 15001 A Coruña, Spain

E. Fernández
Facultad de Ciencias, Universidad de Vigo, 36200 Vigo, Spain

M. Zapata
CIMA, Conselleria de Pesca, Xunta de Galicia,
Apdo 13, 36620 Vilanova de Arousa, Spain

Introduction

Eddies are mesoscale-isolated ecosystems that retain physical, chemical and biological properties, well differentiated from the surrounding environment. Growing evidence accumulated over the past few decades supports the significant role of eddy dynamics upon phytoplankton biomass distribution and production in the oceans (e.g. Jeffrey and Hallegraeff 1980; Angel and Fasham 1983; Falkowski et al. 1991; McGillicudy et al. 1998; Garçon et al. 2001).

Vertical excursions of the pycnocline of several tens of metres can be recognised associated with mesoscale eddy activity (e.g. Richards and Gould 1998). The subsequent environmental changes, mainly nutrient-pumping into the photic layer and modifications of the light field, have the potential to develop favourable or unfavourable conditions for different phytoplankton groups, thus affecting the taxonomic composition and depth distribution of phytoplankton assemblages (e.g. Gould and Fryxell 1988a, 1988b; Olaizola et al. 1993; Smith et al. 1996).

Mesoscale eddy activity in the Bay of Biscay has been the focus of much attention from a physical perspective for the last 20 years (e.g. Madelain and Kerut 1978; Dickson and Hughes 1981; Pingree and Le Cann 1992a). Earlier studies have mainly been focused on descriptions of the slope and shelf currents (Pingree and Le Cann 1989, 1990) and on descriptions of anticyclonic slope water oceanic eddies, named SWODDIES by Pingree and Le Cann (1992a). SWODDIES are mesoscale features of about 50–60 km radius, with an upper core of water warmer and saltier than the adjacent water and

which have been shown to develop from jet-like extensions of the poleward slope current off northern Spain (Cape Ortegal) and the Armorican shelf-break (Pingree and Le Cann 1992a). These authors studied the formation and evolution of three SWODDIES in 1989–1990 using infra-red satellite imagery, and the observations were nicely summarised in a series of sketches (see Fig. 2 in Pingree and Le Cann 1992a). SWODDIES rotate at maximum velocities of about 30 cm s^{-1}, migrating westward at ca. 2 cm s^{-1} over temporal scales of >9 months. During their life-time, anticyclonic SWODDIES are subjected to changes in structure. Sampling of anticyclonic eddy X91 twice over a 3 month period showed a 75% reduction in kinetic energy and angular momentum (Pingree and Le Cann 1992b). In the upper layer their thermohaline structure is characterised by doming of the pycnocline near the eddy centre (Pingree and Le Cann 1992a), which may result in enhanced levels of phytoplankton biomass.

Marker pigments have been widely used in large-scale phytoplankton studies, as they provide qualitative and quantitative data about the composition and distribution of pico–nanoplanktonic groups, which cannot be described in most cases by classic light microscopy and flow cytometry procedures (except for the prokaryotes *Synechococcus* and *Prochlorococcus*; Partensky et al. 1999). A few types of pigments are unequivocally linked to a single phytoplankton group (peridinin and prasinoxanthin in some species of dinoflagellates and prasinophytes), whereas most of them appear distributed among several algal groups (e.g. fucoxanthin derivatives in haptophytes, chrysophytes and dinoflagellates). The application of mathematical algorithms to calculate the relative contribution of phytoplankton groups by combining unique markers with sets of non-specific pigments (CHEMTAX program, Mackey et al. 1996) has been successfully applied in different oceanographic areas to characterise phytoplankton assemblages (e.g. Wright and van den Enden 2000; Rodríguez et al. 2002; Ansotegui et al. 2003).

The local modification of phytoplankton growth conditions, together with the retention of characteristics of slope waters within the eddy, is likely to generate differences in the taxonomic composition of the phytoplankton communities with respect to waters of the Bay of Biscay not affected by these mesoscale features. In order to test this hypothesis, the composition and distribution of phytoplankton assemblages were studied by means of HPLC (high-performance liquid chromatography) pigment analyses and light microscopy in a mesoscale survey conducted across a SWODDY (named eddy AE6).

SWODDY AE6 was initially located, and its evolution subsequently monitored by anomalies in sea-surface temperature (SST) inferred from infra-red AVHRR (advanced very high resolution radiometry) satellite imagery. Two accompanying papers address a detailed description of the physical characteristics of this SWODDY (Gil and Sánchez, submitted) and give an overview of its physical, chemical and ecological properties (Fernández et al., submitted).

Materials and methods

Survey area and sampling

An oceanographic cruise, GIGOVI898, was carried out in the southern Bay of Biscay (45°47′–44°44′N; 7°27′–4°41′W) on board R.V. "Professor Shtokman" from 12 to 31 August 1998. A grid of 141 CTD (conductivity, temperature, depth) stations was visited to define the thermohaline structure of the eddy. Samples were collected for the further quantification of phytoplankton species composition, and the concentration of phytoplankton photosynthetic pigments was determined at 15 selected stations located along two perpendicular transects: N–S transect (stns 31–27) and E–W transect (stns 20–23), and one oblique transect (stns 69–75) (Fig. 1).

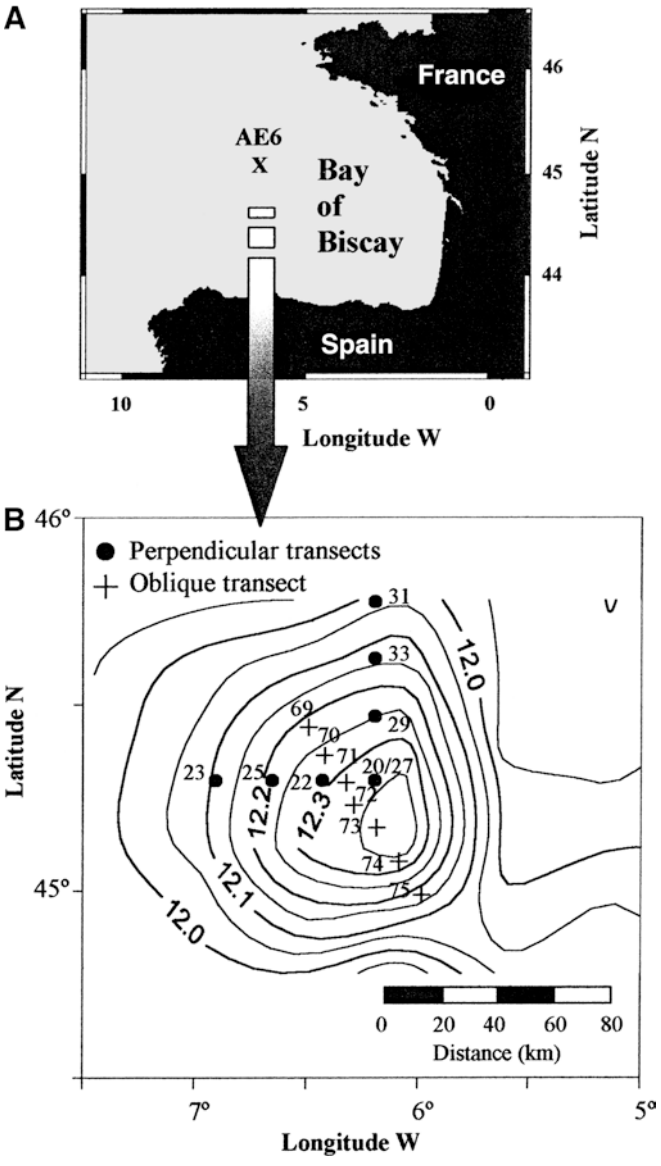

Fig. 1 **A** Study area and **B** distribution of temperature at 200 m depth, with location of phytoplankton/HPLC pigment sampling stations

Vertical profiles of temperature, salinity and fluorescence were obtained with a Neil Brown MARK-III CTD profiler interfaced with a fluorescence sensor. Samples were collected at selected optical depths. Size-fractionated (0.2–2 μm, 2–10 μm and >10 μm) chlorophyll *a* (chl *a*) concentration was measured spectrofluorometrically as described in Teira et al. (2001).

Phytoplankton counting

Aliquots of 125 ml were preserved with Lugol's solution in plastic bottles. Samples were kept in the dark until cell counting; phytoplankton cells were enumerated using the inverted microscope procedures described by Utermöhl (1958). Sample volumes of 10–50 ml were allowed to settle for 24–48 h, depending on the expected abundance of cells as estimated from chl *a* concentrations. A Nikon Diaphot TMD inverted microscope with Nomarski system was used. The whole bottom chamber was examined at ×40 to enumerate larger and less frequent microplankters; then, ×100, ×200, ×400 and ×1000 were used for identifying and counting smaller organisms. Cells were identified to the species level whenever possible, but many of the observed forms had to be placed into taxonomic categories such as small flagellates. Phytoplankton samples for stations located in the oblique transect were not available.

HPLC pigment analysis

Samples for pigment analysis (2.1–6.3 l) were filtered onto 47 mm diameter Whatman GF/F filters and stored at −80°C until further analysis. Frozen filters were extracted in up to 9 ml of 95% methanol using a spatula for filter grinding and further sonication during 5 min at low temperature (~5°C). Extracts were then filtered through 25 mm diameter MFS polypropylene filters (0.20 μm) to remove cell and filter debris. An aliquot (1 ml) of methanol extract was mixed with 0.2 ml of water to avoid peak distortion (Zapata and Garrido 1991). Each sample was injected, just after water addition (200 μl), into a Waters Alliance HPLC system consisting of a 2690 separations module, a Waters 996 photodiode array detector interfaced with a Waters 474 scanning fluorescence detector by a Sat/in analogue interface. Pigment separation was performed by HPLC according to Zapata et al. (2000).

The stationary phase was a C_8 column (symmetry 150×4.6 mm, 3.5 μm particle size, 100 Å pore size) thermostated at 25°C by means of a refrigerated circulator water bath. Mobile phases were: (A) methanol:acetonitrile:aqueous pyridine solution (0.25 M pyridine, pH adjusted to 5.0 with acetic acid) (50:25:25, v/v/v) and (B) acetonitrile:methanol:acetone (60:20:20, v/v/v). A linear gradient from 0% to 40% B was pumped for 22 min, followed by an increase to 100% by 28 min and an isocratic hold at 100% B for a further 12 min. Initial conditions were re-established by reversed linear gradient. Flow rate was 1 ml min^{-1}.

Chlorophylls and carotenoids were detected by diode-array spectroscopy (350–750 nm). Chlorophylls were also detected by fluorescence (excitation: 440 nm, emission: 650 nm). Pigments were identified by co-chromatography with authentic standards (Sigma-Aldrich) and by diode-array spectroscopy (wavelength range: 350–750 nm, 1.2 nm spectral resolution). Each peak was checked for spectral homogeneity using the Millennium^{32} (Waters) software algorithms, and the absorption spectrum was compared with a spectral library previously created. Pigments were quantified by using external standards (collected from macroalgae and phytoplankton cultures by preparative HPLC; Repeta and Bjørnland 1997) and extinction coefficients compiled by Jeffrey et al. (1997).

A statistically significant relationship ($r^2 = 0.87$; $P < 0.001$) was found between HPLC-derived and spectrofluorometrically determined chl *a* concentrations (Fig. 2). The *Y*-intercept of the regression line did not statistically differ from 0, but the slope was < 1, showing that HPLC-derived chl *a* concentrations were higher than those estimated by spectrofluorometry. The observed underestimation of chl *a* by the spectrofluorometric method could arise partially from some interferences with less-fluorescent chlorophyll derivatives as an unknown chl *a* degradation product (discussed later) that appeared widely distributed in this study.

CHEMTAX processing of pigment data

The contribution of algal classes to the total chl *a* concentration was estimated from marker pigments using the chemical taxonomy software CHEMTAX (Mackey et al. 1996) running under MATLAB. Input for the program consisted of a data matrix of pigment concentrations and an initial pigment-ratio matrix; CHEMTAX iteratively optimises the pigment ratios for each algal class to determine the best fit to the observed pigment concentrations.

The initial pigment-ratio matrix (Table 1) was derived from previous analyses performed on several algal cultures belonging to the CIMA (Vilanova, Spain), Instituto Español de Oceanografía

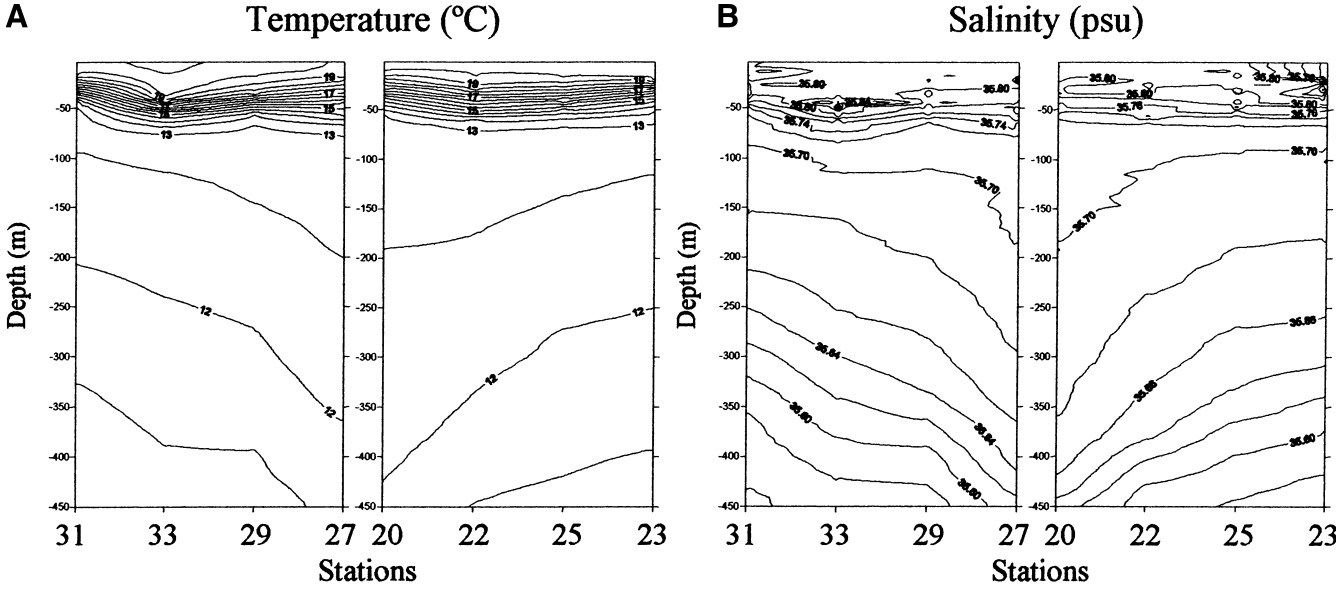

Fig. 2 Vertical distribution of temperature (**A**) and salinity (**B**) in the upper 500 m in the perpendicular transects

Table 1 Initial pigment -ratios and calculated pigment -ratios for GIGOVI 898 cruise analysed by CHEMTAX (*But-fuco* 19′butanoylxyfucoxanthin; *Fuco* fucoxanthin; *Hex-fuco* 19′-hexanoyloxyfucoxanthin; *Perid* peridinin; *Zea* zeaxanthin; *Chl* chlorophyll; *MGDG* monogalactosyldiacylglyceride; *Gyro* gyroxanthin-diester)

	Chl c_3	Chl c_2	But-fuco	Fuco	Hex-fuco	Perid	Zea	Chl b	Chl c_2–MGDG	Gyro	Chl a
Initial pigment- ratio matrix											
Chlorophytes	0.000	0.000	0.000	0.000	0.000	0.000	0.000	0.569	0.000	0.000	1.000
Chrysophytes	0.059	0.129	0.677	0.097	0.000	0.000	0.000	0.000	0.000	0.000	1.000
Cyanobacteria	0.000	0.000	0.000	0.000	0.000	0.000	0.348	0.000	0.000	0.000	1.000
Diatoms	0.000	0.183	0.000	0.754	0.000	0.000	0.000	0.000	0.000	0.000	1.000
Dinoflagellates I	0.000	0.233	0.000	0.000	0.000	0.444	0.000	0.000	0.000	0.000	1.000
Dinoflagellates II	0.056	0.086	0.093	0.030	0.153	0.000	0.000	0.000	0.000	0.043	1.000
Haptophytes	0.111	0.203	0.000	0.007	0.543	0.000	0.000	0.000	0.156	0.000	1.000
Output pigment- ratio matrix											
Chlorophytes	0.000	0.000	0.000	0.000	0.000	0.000	0.000	0.569	0.000	0.000	1.000
Chrysophytes	0.059	0.129	0.677	0.097	0.000	0.000	0.000	0.000	0.000	0.000	1.000
Cyanobacteria	0.000	0.000	0.000	0.000	0.000	0.000	0.495	0.000	0.000	0.000	1.000
Diatoms	0.000	0.183	0.000	0.754	0.000	0.000	0.000	0.000	0.000	0.000	1.000
Dinoflagellates I	0.000	0.233	0.000	0.000	0.000	0.444	0.000	0.000	0.000	0.000	1.000
Dinoflagellates II	0.089	0.086	0.093	0.030	0.153	0.000	0.000	0.000	0.000	0.043	1.000
Haptophytes	0.152	0.422	0.000	0.009	0.653	0.000	0.000	0.000	0.121	0.000	1.000

(IEO, Vigo, Spain) and the CSIRO Culture Collection (Hobart, Australia). The initial ratio matrix included seven algal categories defined by pigment signatures consisting of five chlorophylls and six carotenoids: "chlorophytes": chl *b*; "chrysophytes": chl c_3, chl c_2, 19′-butanoyloxyfucoxanthin (But-fuco), fucoxanthin (Fuco); "cyanobacteria": zeaxanthin (Zea); "diatoms": chl c_2 and Fuco; "dinoflagellates I": chl c_2, peridinin (Perid); "dinoflagellates II": chl c_3, chl c_2, Fuco, 19′-hexanoyloxyfucoxanthin (Hex-fuco), gyroxanthin-diester (Gyro; Millie et al. 1997; Bjørnland et al. 2000), and "haptophytes": chl c_3, chl c_2, But-fuco, Fuco, Hex-fuco, chl c_2–monogalactosyldiacylglyceride (chl c_2–MGDG; Garrido et al. 2000).

Results

Thermohaline properties of the SWODDY

The distribution of temperature at the 200 m isobath (Fig. 1) shows the central core of warm water characteristic of SWODDIES (Pingree and Le Cann 1992a, 1992b) located approximately at 45°40′N; 6°40′W. Temperature at 200 m changed from 12°C outside the eddy to 12.4°C at the centre, over a horizontal scale of 50–60 km. This thermal gradient in subsurface waters indicated progressive depression of isotherms towards the eddy centre, indicating anticyclonic rotation of the mesoscale structure.

The geostrophic velocity field at AE6 revealed its anticyclonic motion down to 1500 m, with highest velocities (>10 cm s^{-1}) measured in the upper 300 m, ca. 20 km away from the eddy centre (Fernández et al., submitted). This region will be referred to hereafter as the high-velocity region, corresponding to stns 25 and 29 (perpendicular transects) and stns 70 and 74 (oblique transect).

Figure 2 shows the vertical distribution of temperature (Fig. 2A) and salinity (Fig. 2B) along the two perpendicular transects, illustrating the thermohaline structure of the anticyclonic eddy AE6. Temperature profiles clearly showed deepening of isotherms at the eddy centre (below 200 m), while in the upper tens of metres shoaling of isotherms was apparent. A homogeneous, high-salinity (ca. 35.70), central core typical of SWODDIES was also clearly manifested.

Fluorometrically derived chl *a* distribution

The vertical position of the subsurface chlorophyll maximum (SCM) (Fig. 3) was closely related to the upward doming of the thermocline. Outside the eddy, the SCM was located at 60–70 m, whereas at the eddy centre it was found shallower (40 m at stn 20) and showed higher chl *a* concentrations (stn 20: 610 ng chl *a* l^{-1}; stn 23: 270 ng chl *a* l^{-1}). Surface chl *a* values were uniformly low at all sampling stations (<70 ng chl *a* l^{-1}). In the oblique transect similar features were registered (Fig. 3). However, chl *a* showed a slight increase at the eddy centre (stn 72: 560 ng chl *a* l^{-1}) as compared with the surrounding waters (stn 69: 390 ng chl *a* l^{-1}). Picoplankton (<2 μm cells) accounted for $48.4 \pm 10.7\%$ of total chl *a* concentration. The two larger size-classes, 2–10 μm and >10 μm cells, contributed $24.1 \pm 6.5\%$ and $23.7 \pm 8.7\%$, respectively.

Phytoplankton cell counts

Figure 4 shows phytoplankton cell counts obtained in the two perpendicular transects. Unidentified flagellates (8–10 μm cell size), dinoflagellates and diatoms were the most abundant algal groups. Flagellates and dinoflagellates (*Cachonina halli* and unidentified dinoflagellates <30 μm cell size) reached their absolute maximum abundance inside the eddy (stn 22, 50 m depth; 270 flagellates ml^{-1} and 532 dinoflagellates ml^{-1}) in accordance with the absolute maximum of chl *b* and chl c_3, while

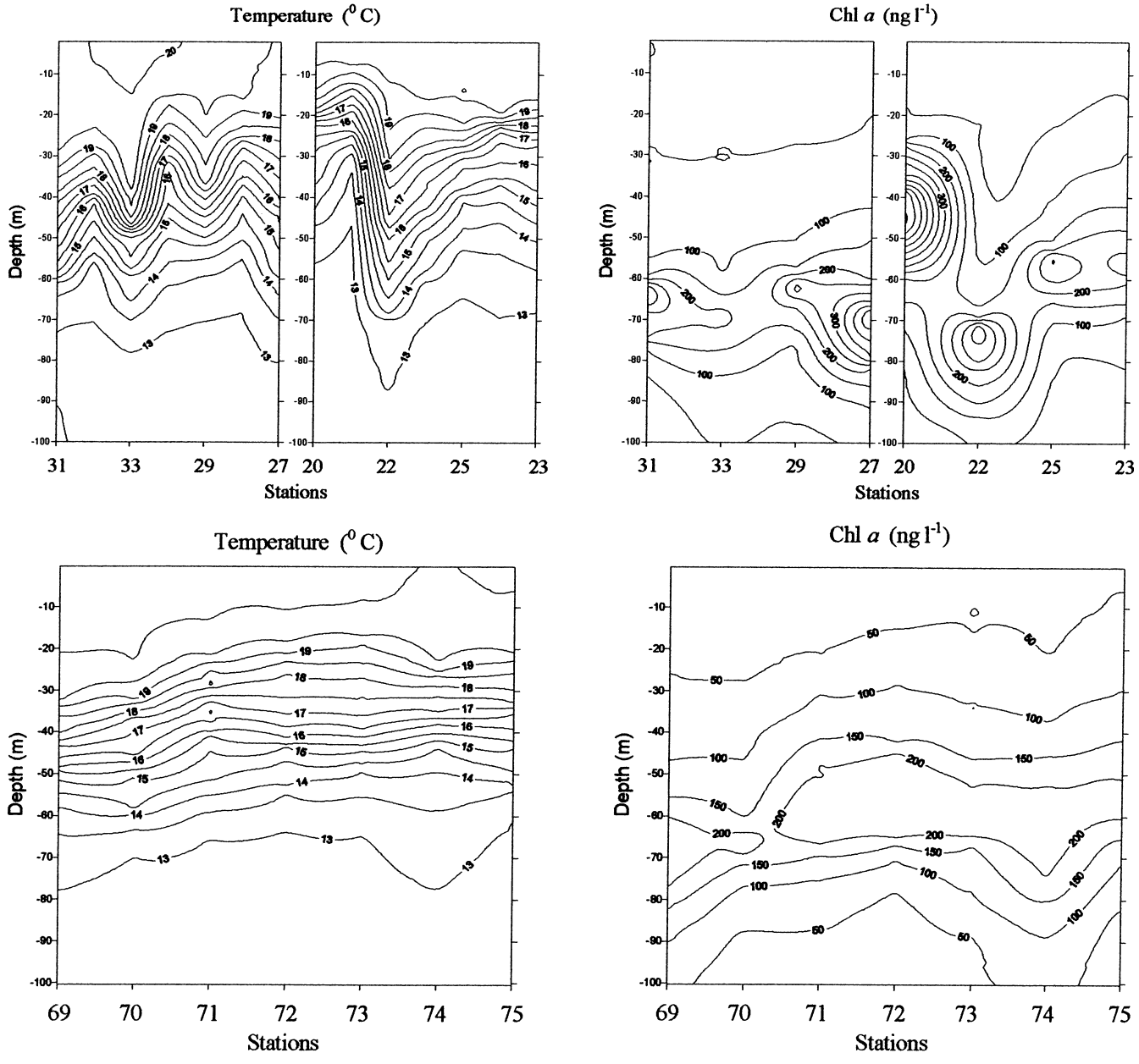

Fig. 3 Vertical distribution of temperature and fluorometrically derived chlorophyll *a* concentrations in the upper 100 m: perpendicular transects (*upper panels*) and oblique transect (*lower panels*)

peridinin concentrations did not show significant spatial variations in spite of the relatively high contribution of dinoflagellates observed at the eddy centre.

Diatoms were almost entirely restricted to the eddy centre, the dominant species being *Pseudo-nitzschia delicatissima*, with an absolute maximum at stn 20 (45 m depth; 519 cells ml^{-1}), coinciding with the highest chl *a* values measured during the study. Other phytoplankton groups such as chrysophytes, cryptophytes and haptophytes never exceeded densities of 50 cells ml^{-1}. Chrysophyceae, mainly *Dictyocha speculum* and *Solenicola setigera*, showed their absolute maximum at stn 29 inside the eddy (40 m depth; 15 cells ml^{-1}), as well as at the eddy centre (stns 27 and 20). Cryptophytes showed an absolute maximum at 40 m depth inside the eddy (stn 22; 43 cells ml^{-1}) and high densities in surface waters of stn 33. The marker pigment Allo was only detected in trace amounts at the chl *a* maximum of the eddy centre, and for this reason it has not been included in CHEMTAX data processing. Haptophytes were very scarce, and their maximum densities were reached outside the eddy above 20 m depth (stn 31).

HPLC-derived pigment distributions

Samples for the further determination of pigment concentrations by HPLC were collected from the two perpendicular transects (stns 23–20 and 27–31), and the oblique transect (stns 69–75) (see Fig. 1). Upper-layer

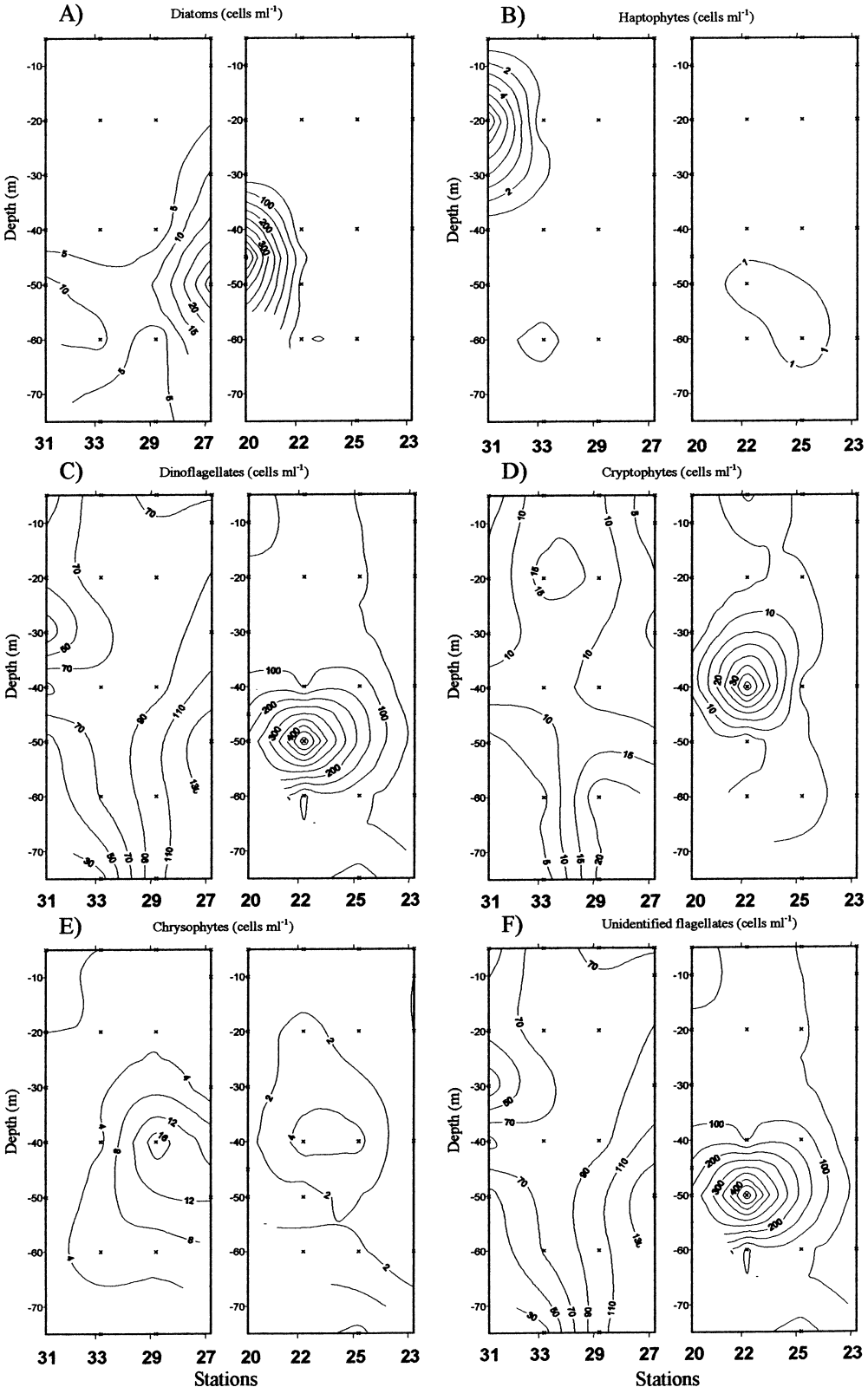

Fig. 4 Vertical distribution of the abundance of phytoplankton groups (cells ml^{-1}) in the perpendicular transects: **A** diatoms, **B** haptophytes, **C** dinoflagellates, **D** cryptophytes, **E** chrysophytes and **F** unidentified flagellates

(< 20 m) chl *a* concentrations (Fig. 5A) were low in both transects (14–68 ng l^{-1}), with maximum values detected between 40 and 60 m depth (23–780 ng l^{-1}). The main accessory chlorophylls detected (Fig. 4B–D) were chl *b* (4–122 ng l^{-1}), chl c_2 (1–104 ng l^{-1}), chl c_3 (0–32 ng l^{-1}) and chl c_2–MGDG (0–15 ng l^{-1}). The main chl c_2–MGDG detected in this study resembled the chromatographic properties and visible spectrum of a chl c_2–MGDG (14:0/14:0) recently described in several *Chrysochromulina* species (Zapata et al. 2001). Lower

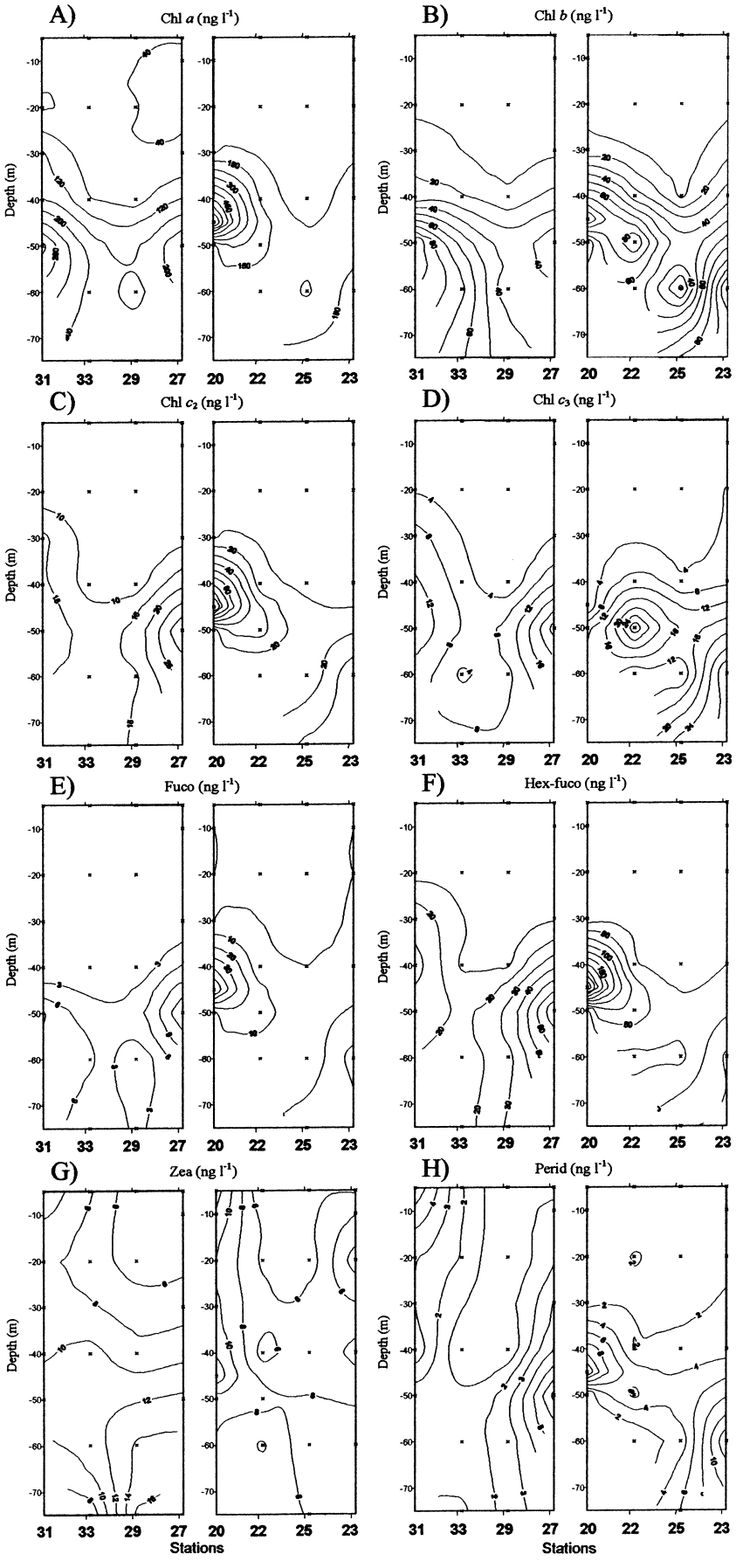

Fig. 5 Vertical distribution of the concentrations (ng l^{-1}) of chlorophylls and carotenoids in the perpendicular transects: **A** chl *a*, **B** chl *b*, **C** chl c_2, **D** chl c_3, **E** fucoxanthin (*Fuco*), **F** 19′-hexanoyloxyfucoxanthin (*Hex-fuco*), **G** zeaxanthin (*Zea*) and **H** peridinin (*Perid*)

amounts of other chl c_2–MGDGs similar to that described in *Emiliania huxleyi* (Garrido et al. 2000), with fatty acid residues (14:0/18:4), were also detected in a series of samples, mainly located at the eddy centre. An unknown chl *a* degradation product showed a widespread vertical distribution outside and inside the high-velocity region, being more abundant than chl *a* in some cases (up to 1101 ng l^{-1}; for quantification purposes we assumed the same molar extinction coefficient as for chl *a*). Its visible spectrum resembled that of a linear tetrapyrrole as it lacked the absorption peak above 600 nm (single absorption peak at 430 nm in HPLC eluent), indicating that the chlorophyll haem ring had been broken (Porra et al. 1997).

The carotenoid composition in the study area was mainly constituted by several fucoxanthin-related pigments, Hex-fuco: 0–275 ng l^{-1}, Fuco: 0–61 ng l^{-1} and But-fuco: 0–34 ng l^{-1}, Zea: 0–26 ng l^{-1}, and Perid: 0–14 ng l^{-1}. Trace values (< 5 ng l^{-1}) of Gyro, alloxanthin (Allo), violaxanthin (Viola), lutein (Lut) and prasinoxanthin (Pras) were also detected.

Perpendicular transects

The distribution patterns of chl *a* and chl c_2 (Fig. 5A, C) were quite similar, showing their maximum concentrations between 40 and 50 m depth at the eddy centre (Stns 27 and 20). In addition, chl *a* also showed a distinct maximum at stn 31 located outside the eddy. A slightly different pattern emerged from the spatial distribution of chl *b* and chl c_3, showing maxima at 50 m depth at stn 22 located inside the eddy (Fig. 5B, D). Chl c_2–MGDG followed a similar distribution to chl c_2, reaching maximum values inside the eddy (stns 27 and 20; not shown).

The distributions of fucoxanthin and its acyloxy-derivatives Hex-fuco and But-fuco (not shown) were quite similar, and their maximum concentrations were observed at the eddy centre (stns 20 and 22) between 40 and 50 m depth (Fig. 5E, F). Zeaxanthin also showed higher concentrations at the eddy centre, but values close to 10 ng l^{-1} were measured at all sampling stations between 30 and 75 m depth (Fig. 5G). Peridinin was generally restricted to the eddy centre corresponding with the chl *a* maximum, but also showed a maximum at 60 m depth at stn 23 located outside the eddy (Fig. 5H).

Oblique transect

Chl *a* and chl c_2 followed quite similar vertical distributions (Fig. 6A, C), with three areas of relatively high pigment concentrations: at stn 69 (70 m depth) located outside the eddy and at stns 72 (45 m depth) and 73 (60 m depth) located inside the eddy. Chl *b* and chl c_3 showed additional maxima at stns 74 and 75 (Fig. 6B, D) located at the high geostrophic velocity area and outside the eddy structure, respectively. Chl c_2–MGDG showed its maximum concentrations between stns 72 and 75 at 45–65 m depth.

Fucoxanthins showed the same distribution pattern (Fig. 6E, F), with relatively high concentrations below 40 m depth, especially from stns 72 (40 m depth) to 75 (60 m depth); maximum concentrations were observed inside the eddy (stns 72 and 73). Zeaxanthin concentrations, although slightly lower than in the perpendicular transects, showed maximum values at stns 72–75 (Fig. 6G), reaching an absolute maximum outside the eddy (stn 75). Peridinin registered its highest values at the eddy centre (Fig. 6H). Relatively high concentrations were also observed from 30 to 60 m depth at stns 69–75.

Pigment ratios along vertical profiles

The vertical distribution of pigment ratios (i.e. concentration of accessory pigments normalised to chl *a*) did not show a clear trend; only chl *b*:chl *a* ratios showed a significant positive relationship with depth ($r = 0.60$, $P < 0.001$, $n = 74$). However, carotenoid ratios such as those for But-fuco, Fuco and minor pigments such as violaxanthin (Viola), lutein (Lut) and prasinoxanthin (Pras) increased significantly with depth (But-fuco: $r = 0.36$, $P < 0.005$, $n = 74$; Fuco: $r = 0.63$, $P < 0.001$, $n = 74$; Viola: $r = 0.43$, $P < 0.001$, $n = 74$; Lut: $r = 0.52$, $P < 0.001$, $n = 74$; Pras: $r = 0.47$, $P < 0.001$, $n = 74$). Although, in the case of Viola, Lut and Pras these were only detected occasionally between 40 and 60 m depth, mainly outside the eddy in both transects. Zeaxanthin was the unique exception to this pattern, as its pigment ratio to chl *a* decreased with depth ($r = 0.61$, $P < 0.001$, $n = 74$).

The relative contribution of chl c_3 to the total pool of chl *c* (chl c_3 + chl c_2 + chl c_2–MGDG) increased with depth ($r = 0.62$, $P < 0.001$, $n = 74$). Similarly, But-fuco and Fuco showed a higher relative contribution to the total pool of fucoxanthin (Fuco + Hex-fuco + But-fuco) with depth (But-fuco: $r = 0.79$, $P < 0.001$, $n = 74$; Fuco: $r = 0.74$, $P < 0.001$, $n = 74$), while Hex-fuco followed an opposite trend ($r = -0.85$, $P < 0.001$, $n = 74$).

Pigment patterns

Typical pigment patterns at the SCM are illustrated by means of three selected chromatograms (Fig. 7A–C) obtained from the high-velocity region, central, and surrounding waters outside the SWODDY. Fucoxanthin and Hex-fuco were the main carotenoids at the eddy centre, whereas at the edge and outside the eddy a higher contribution of Zea, Perid and chl *b* was detected. For comparison purposes a chromatogram obtained from a sample collected off the northwest coast of Spain is also represented (Fig. 7D), showing the close similarity in pigment composition between phytoplankton assemblages characteristic of SWODDY AE6 and those corresponding to the poleward current from which these mesoscale structures are ultimately derived. The main differences were due to the detection of Allo and divinyl (DV) chl *a* and DV chl *b* in the slope current, indicating

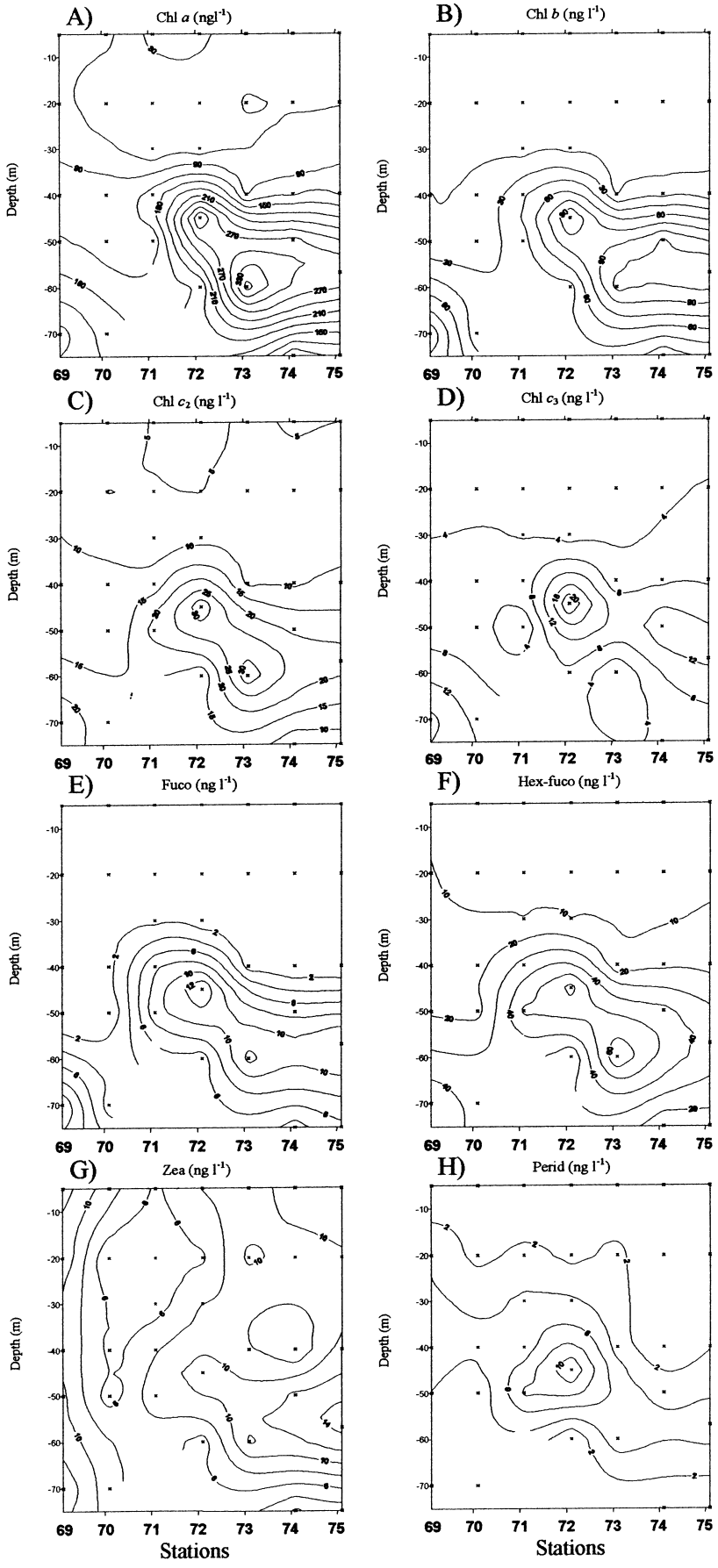

Fig. 6 Vertical distribution of the concentrations (ng l^{-1}) of chlorophylls and carotenoids along the oblique transect: **A** chl *a*, **B** chl *b*, **C** chl c_2, **D** chl c_3, **E** fucoxanthin (*Fuco*), **F** 19′-hexanoyloxyfucoxanthin (*Hex-fuco*), **G** zeaxanthin (*Zea*) and **H** peridinin (*Perid*)

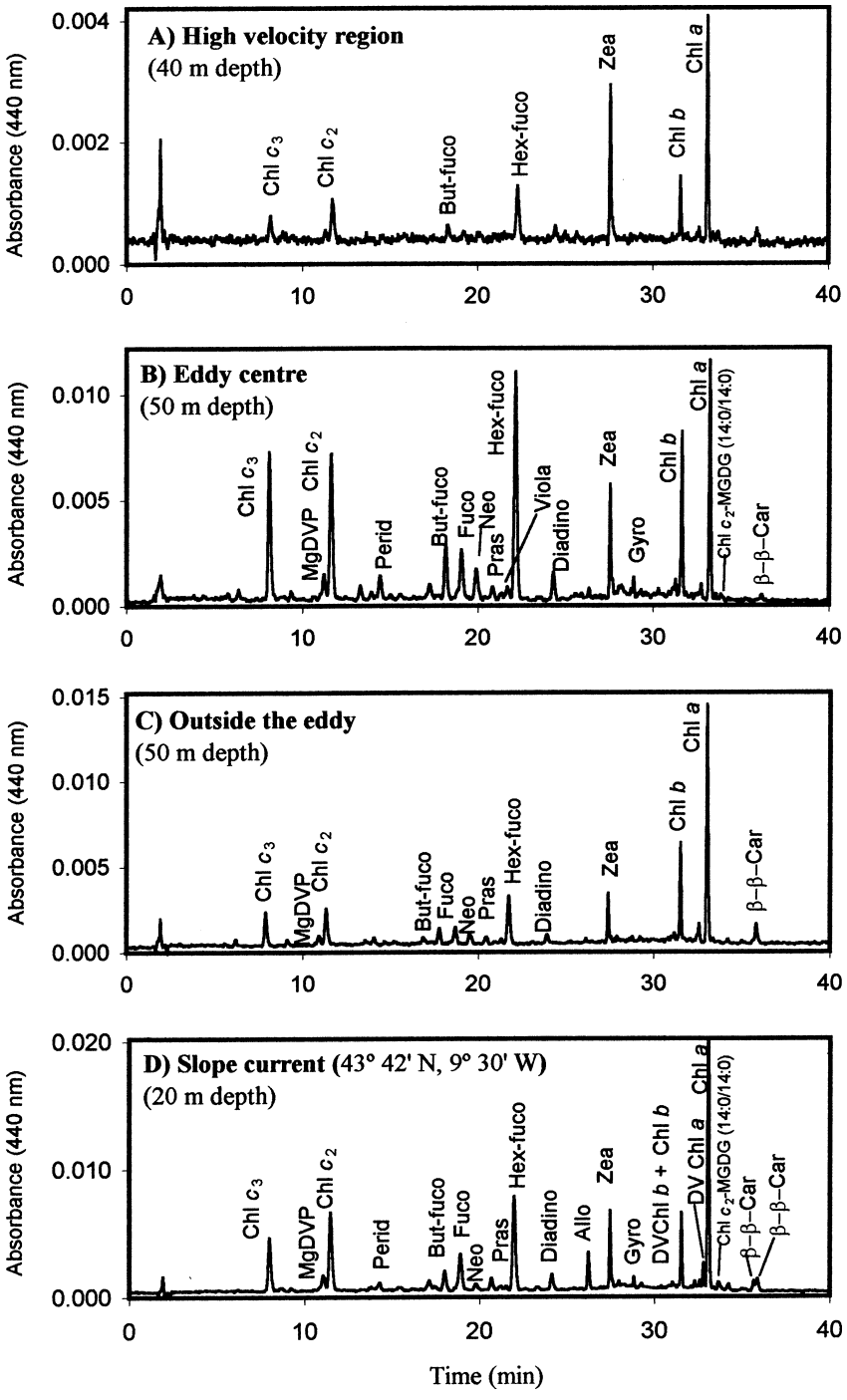

Fig. 7 Selected chromatograms showing the pigment patterns associated with different sampling regions: **A** high-velocity region, **B** eddy centre and **C** outside eddy. For comparative purposes a chromatogram (**D**) illustrating the pigment composition obtained from the slope current off northwest Spain in October 1999 is also shown

the presence of cryptophytes and the cyanobacteria *Prochlorococcus marinus*, whereas those pigments were not found in phytoplankton samples from SWODDY AE6.

CHEMTAX analysis of HPLC pigment data

Seven pigment-based "algal categories" were defined to reconstruct phytoplankton assemblages in the study area: "chlorophytes", "chrysophytes", "cyanobacteria", "haptophytes", "diatoms", "dinoflagellates I" and "dinoflagellates II" (which contain haptophyte-like pigments and gyroxanthin-diester). The vertical distribution of CHEMTAX groups (Figs. 8, 9) provided an alternative view of the phytoplankton community structure to that obtained from direct observation with light microscopy.

Perpendicular transects

"Chlorophytes", "haptophytes" and "dinoflagellates II" were the most abundant groups at almost all sampling stations (Fig. 8E, B, G). Their maximum values were

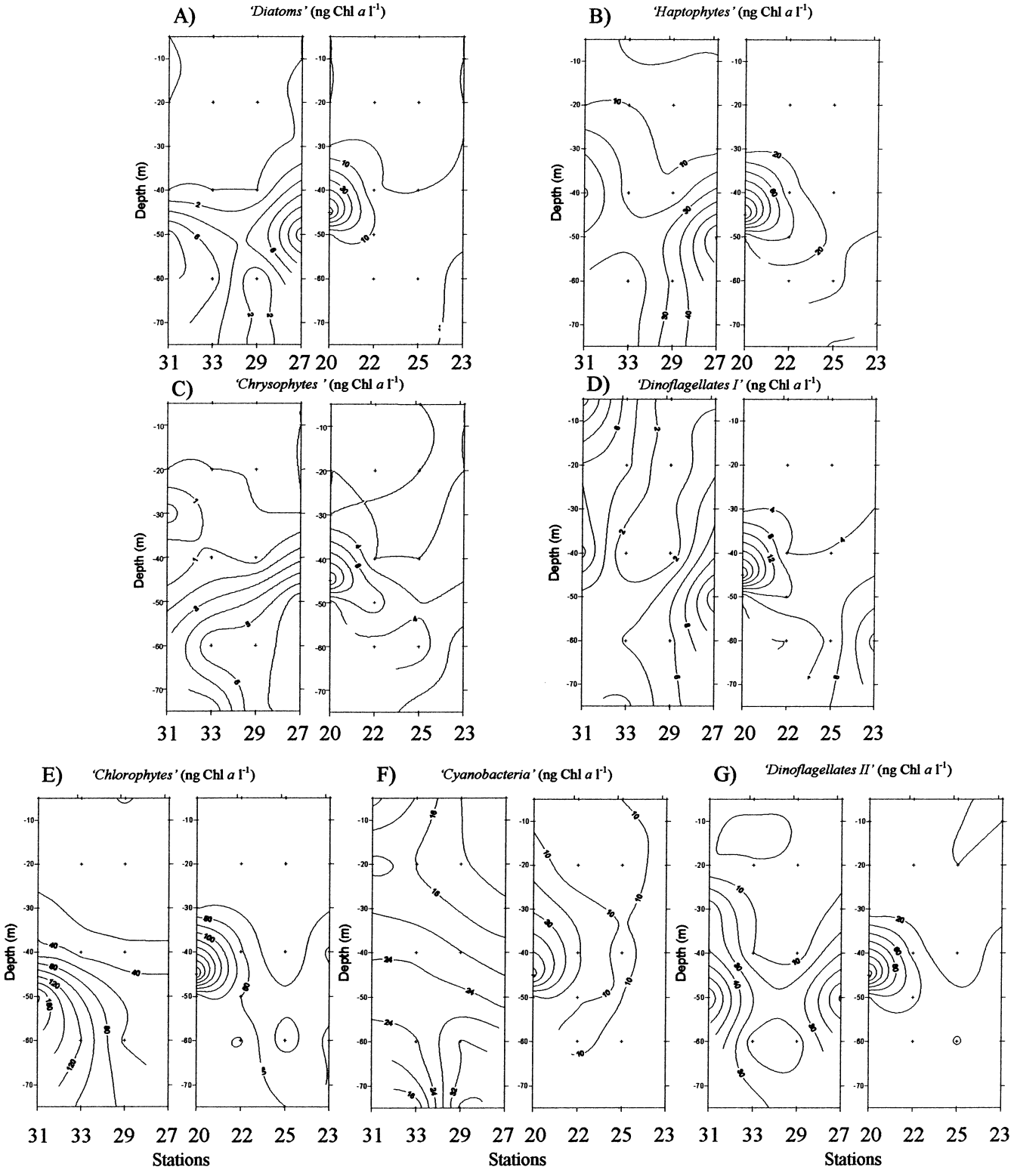

Fig. 8 Vertical distribution of CHEMTAX-derived phytoplankton groups (ng chl a l^{-1}) in the perpendicular transects: **A** "diatoms", **B** "haptophytes", **C** "chrysophytes", **D** "dinoflagellates I", **E** "chlorophytes", **F** "cyanobacteria", **G** "dinoflagellates II"

observed at the eddy centre (stns 27 and 20), although "chlorophytes" and "dinoflagellates II" also showed high abundances outside the eddy (stn 31).

The contribution of "diatoms" to chl a, as interpreted by CHEMTAX, closely resembled the distribution of diatom abundance derived from microscopic counts, confirming the presence of this taxonomic group almost confined to the eddy centre (stns 27 and 20). "Diatoms" were also present, although with lower abundance, at subsurface layers outside the eddy

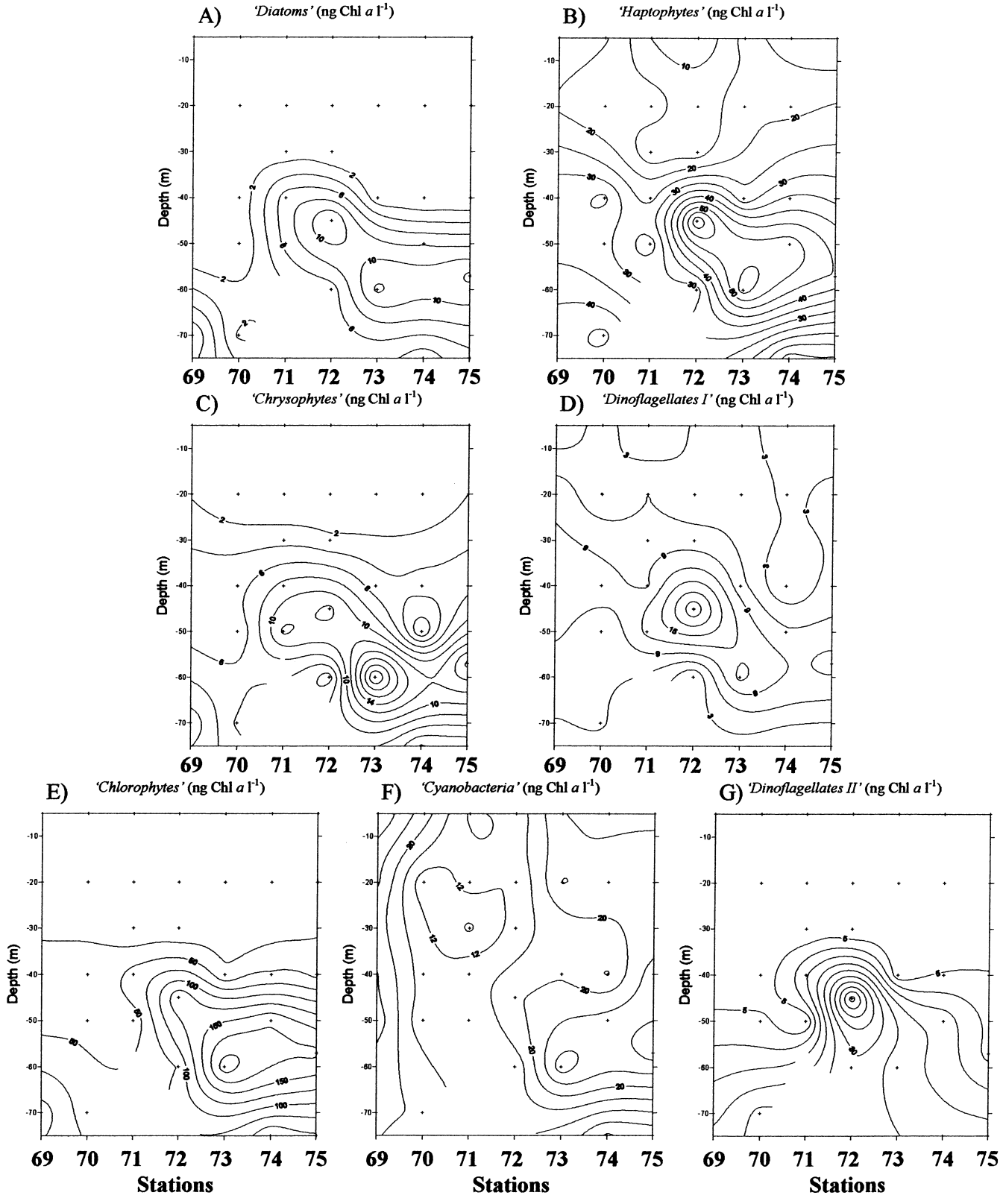

Fig. 9 CHEMTAX-derived phytoplankton groups (ng chl *a* l^{-1}) in the oblique transect from the GIGOVI898 cruise: **A** "diatoms", **B** "haptophytes", **C** "chrysophytes", **D** "dinoflagellates I", **E** "chlorophytes", **F** "cyanobacteria", **G** "dinoflagellates II"

(stns 31 and 23). "Dinoflagellates I" and "chrysophytes" showed their maximum concentrations between 40 and 60 m depth at stns 20 and 22, resembling the

distribution patterns of Hex-fuco, chl c_2 and chl c_3. The highest abundance of dinoflagellates as estimated from optical microscopy was not paralleled by increased concentrations of chl *a* contributed by "dinoflagellates I", as the marker pigment peridinin did not follow the same spatial pattern depicted by cell counts.

The interpreted contribution of "cyanobacteria" to chl *a* was quite similar throughout the water column along the section between stns 31 and 27, with highest values below 30 m depth. At the western section (stns 20–23) an absolute maximum at the eddy centre and high contributions of "cyanobacteria" below 60 m depth were observed.

Oblique transect

The most abundant algal classes as estimated from their contribution to chl *a* were the "chlorophytes" and "haptophytes". These groups showed maximum abundance at stn 72 coinciding with all the algal groups estimated by CHEMTAX, but different distributions at stns 73 and 74 resembling the distribution patterns of chl *b* and chl c_3 (Fig. 9). "Diatoms" and "chrysophytes" were scarce, only being detected below 40 m depth and mainly at the eddy centre (stns 72–73). "Dinoflagellates I" showed an absolute maximum at the eddy centre and higher concentrations below 40 m depth, although they were also found up to 20 m depth along a section between stns 69 and 72. The relative contribution of "dinoflagellates II" was much lower than in the perpendicular transects, and their distribution was similar to that of "dinoflagellates I". "Cyanobacteria" showed a widespread vertical distribution throughout the water column as compared with the rest of the phytoplankton groups. Their maximum values were observed mainly outside the eddy (stns 69 and 75) and also at stn 73 inside the eddy.

Phytoplankton composition and pigments versus sampling location

A nested analysis of variance (ANOVA) was performed to determine the effect of: (1) sampling depth (upper: 5–30 m, intermediate: 40–60 m and deep: 75–100 m), (2) eddy regions (central, outside and high-velocity region) and (3) stations, on the distribution of phytoplankton assemblages detected both from microscopic counts and pigments. Sampling depth represented the main effect upon the distribution of most pigments and the taxonomic distribution of phytoplankton groups. Only a reduced number of variables (e.g. dinoflagellate and flagellate cell counts in the perpendicular transects and size-fractionated chl *a* in the oblique transect) were significantly influenced by the eddy region.

Significant differences among sampling stations were not observed. Significant effects due to sampling depth were expected, because, as previously mentioned, the upper layer (5–20 m) showed the lowest phytoplankton abundance (< 70 ng chl *a* l^{-1}), independent of sampling location, whereas the highest phytoplankton densities and pigment concentrations were observed at the SCM depth (40–60 m). Thus, a new ANOVA was performed using only the averaged pigments and phytoplankton composition determined by cell counts and CHEMTAX at the SCM (Table 2), with an aim to reveal the main differences in phytoplankton composition related to the eddy thermohaline structure.

Microscopic counts showed the existence of a phytoplankton community dominated by dinoflagellates, diatoms and flagellates at the eddy centre, whereas among CHEMTAX groups, only "cyanobacteria" showed a distinct spatial distribution regarding sampling location in the oblique transect. "Chlorophytes" were the most abundant pigment-based algal group at all sampling stations. In the perpendicular transects, at the eddy centre, "chlorophytes", "haptophytes" and "dinoflagellates II" accounted for 35%, 20% and 24% of total chl *a*, respectively, while "diatoms" only represented 10%. In the high-velocity region "cyanobacteria" reached up to 20% of total chl *a*, whereas "dinoflagellates II" reached their minimum proportion.

Outside the eddy (in the perpendicular transect) and at all sampling stations in the oblique transect, the highest contributions of "chlorophytes" (up to 50% of total chl *a*) were observed, with "cyanobacteria" and "haptophytes" accounting for approximately 30% of total chl *a* in the oblique transect. "Dinoflagellates I" and "chrysophytes" always constituted $< 10\%$ of total chl *a*. A reduced contribution of picoplanktonic organisms at the eddy centre (44.5–50.3% total chl *a* in both transects) as compared with outside (53.9–61.1%) and the high-velocity (48.8–55.8%) region was consistently observed in all transects. The main differences in chl *a* concentration were observed in the perpendicular transects, where it showed higher values at the eddy centre. The lowest pigment concentrations were observed at stations located in the high-velocity region.

Although chl *a* values were significantly higher at the eddy centre only in the perpendicular transects, the main differences in the concentration of accessory pigments were detected in the oblique transect, where But-fuco, Perid and Zea were more abundant at the eddy centre. Pigment ratios of chl c_3, chl c_2 and fucoxanthin-related pigments were significantly higher at the eddy centre in the oblique transect.

Discussion

Several studies have focussed on the changes induced by eddies upon the composition and production of phytoplankton assemblages (Fryxell et al. 1985; Lochte and Pfannkuche 1987; Gould and Fryxell 1988a, 1988b; Olaizola et al. 1993; among others). These studies show that the vertical location, magnitude and composition of the chlorophyll maximum can be highly affected by changes in vertical nutrient transport and oscillations of

Table 2 Averaged concentrations of pigments and phytoplankton composition at the SCM (40–60 m depth) at three sampling regions (eddy centre, high velocity region, and surrounding waters). ANOVA probability results (*P*) due to sampling regions are also shown (*n.s.* not significant)

Pigment concentration (ng l^{-1})	Perpendicular transects			ANOVA (*P* value)	Oblique transect			ANOVA (*P* value)
	Outside	Centre	High velocity		Outside	Centre	High velocity	
Chl c_3	15.6	11.7	8.1	n.s.	8.9	9.0	7.0	n.s.
Chl c_2	18.4	31.0	13.1	n.s.	14.8	15.1	10.3	n.s.
But-fuco	7.7	10.3	4.7	n.s.	6.7	6.9	2.5	<0.05
Fuco	7.6	14.4	3.3	n.s.	5.2	6.0	2.0	n.s.
Hex-fuco	39.0	70.2	22.8	n.s.	25.6	29.2	18.4	n.s.
Perid	5.0	4.8	2.1	n.s.	3.3	6.3	1.9	<0.05
Zea	10.4	12.1	10.6	n.s.	10.5	8.0	5.8	<0.025
Chl *b*	57.9	50.0	38.5	<0.05	51.6	42.2	33.2	n.s.
Chl c_2–MGDG (14:0/14:0)	1.3	3.0	1.3	n.s.	3.5	3.2	3.4	n.s.
Chl *a*	185.6	228.0	121.7	<0.001	160.7	135.0	120.2	n.s.
Unknown chl *a* degradation product	85.3	40.1	60.3	n.s.	92.6	14.0	55.7	n.s.
Pigment-based phytoplankton groups (ng chl *a* l^{-1})								
Chlorophytes	59.2	43.4	43.1	n.s.	57	59.3	60.4	n.s.
Chrysophytes	4.8	1.2	4.5	n.s.	4.7	5.3	3.6	n.s.
Cyanobacteria	12.4	9.2	21.2	n.s.	14.5	9.7	11.6	n.s.
Diatoms	4.6	12.2	4.3	n.s.	2.7	4.1	1.5	n.s.
Dinoflagellates I	2.2	2.2	5.5	n.s.	3.9	4.5	2.9	n.s.
Dinoflagellates II	13.3	31.1	9.5	n.s.	7.7	9.2	4.6	n.s.
Haptophytes	14.4	25.9	17.6	n.s.	15.2	14.5	19	n.s.
Cell counts (cells ml^{-1})								
Chrysophyceae	0.1	3.5	5.3	n.s.				
Cryptophytes	4.2	8.7	9.9	n.s.				
Diatoms	3.2	89.2	2.6	<0.01				
Dinoflagellates	32.3	162.6	84.6	<0.001				
Flagellates	16	93.3	39.6	<0.01				
Haptophytes	0.8	0.3	0.4	n.s.				

the pycnocline associated with mesoscale structures. Gould and Fryxell (1988a) summarised some similarities observed among cyclonic eddies from the North Pacific, Gulf Stream and East Australian Current, showing that the rings usually developed enhanced phytoplankton biomass (particularly diatoms), which was frequently found to concentrate in the central regions of the mesoscale structure (Hitchcock et al. 1985).

The results obtained in the present study showed that SWODDY AE6 developed higher chl *a* values (by a factor of two) and lower contributions of picoplankton to total chl *a* (44–50% and 54–61%, SCM values at the eddy centre and outside the eddy, respectively) than those observed in the surrounding waters. Enhanced phytoplankton biomass at AE6 is related to the doming of the pycnocline at the eddy centre (Pingree and Le Cann 1992a). The injection of nutrients into a well-illuminated SCM, mainly driven by the passage of internal waves, has been hypothesised to induce the establishment of favourable conditions for phytoplankton growth (Fernández et al., submitted).

Microscopic counts showed that the spatial distributions of some groups as diatoms, dinoflagellates and flagellates were significantly influenced by the mesoscale structure, whereas HPLC pigment analysis failed to detect these spatial trends. However, pigment analysis indeed provided a more sensitive technique to infer the phytoplankton composition of picoplankton groups.

Thus, pigment-based interpretation of algal groups showed that characteristic phytoplankton assemblages inside the SWODDY were "chlorophytes", "haptophytes" and "dinoflagellates II", whereas "chlorophytes" and higher relative contributions of "cyanobacteria" (type *Synechococcus*) were detected in the surrounding waters. Marked differences between microscopically and pigment-derived abundances of large-sized phytoplankton groups were also obtained. Hence, dinoflagellates showed maximum abundance at the eddy centre (stn 22), which was not paralleled by the distribution of HPLC-derived pigments. These discrepancies can be related to the high fraction of heterotrophic dinoflagellates found in this region (particularly at stn 22). In addition, the most abundant photosynthetic dinoflagellates in this study were estimated to display haptophyte-like pigments("dinoflagellates II"), whereas peridinin-containing dinoflagellates("dinoflagellates I") were a minority. The pigment class "dinoflagellates II" includes those species with "haptophyte-like pigments", such as *Gymnodinium breve* (Bjørnland 1990) and *Gyrodinium galatheanum* (Johnsen and Sakshaug 1993; Bjørnland et al. 2000), renamed *Karenia brevis* and *Karlodinium micrum*, respectively (Daugbjerg et al. 2000), differentiated from the pigment class "haptophytes" due to their marker pigment gyroxanthin-diester (Millie et al. 1997; Örnólfsdóttir et al. 2003). Although it was detected in minor amounts, the wide distribution of

gyroxanthin-diester in this study opens the question as to whether other pico–nanoeukaryotes besides dinoflagellates could have also contributed to "dinoflagellates II".

Microscopic cell counts and HPLC-derived pigments showed that diatoms were almost entirely restricted to the eddy centre, although their relative contribution to chl *a* remained low. On the other hand, chl c_1 has not been detected in those samples with higher abundance of diatoms. The dominant species, *Pseudo-nitzschia delicatissima*, has been reported to contain chl c_1 (Zapata, personal communication). Although, its relative content in this species is fairly low and it would explain the failure to detect chl c_1 even at the maximum of *P. delicatissima* at the eddy centre.

Cryptophytes were detected in low cell numbers by microscopic counting. Their marker pigment, alloxanthin, was only measured in trace amounts at the SCM at the eddy centre, suggesting also the existence of a heterotrophic component in this group. Both techniques also yielded a distinct view when other algal groups were considered. These discrepancies are probably related to the large fraction of pico–nanoplankton that cannot be identified by means of light microscopy and, for the most part, are included in the unidentified flagellate group. Based on the marker pigments detected, these flagellates would mainly belong to algal classes such as chlorophytes, cryptophytes, haptophytes and pelagophytes. The chl *b* distribution observed during this study was not paralleled by significant contributions of violaxanthin, lutein or prasinoxanthin. This result shows that prasinoxanthin-containing prasinophytes were indeed a minor group in this study, as prasinoxanthin appeared only in a few samples, mainly at the SCM outside the eddy.

The distribution of "haptophytes" was reconstructed including in its pigment composition a chl c_2–MGDG with the same chromatographic properties as that described by Zapata et al. (2001). This compound is a marker pigment for *Chrysochromulina* species, and, although with low concentration (< 15 ng l^{-1}), its widespread spatial distribution suggests that *Chrysochromulina* spp. were an abundant component of the haptophytes in the present study. The discrepancies observed between microscopic results and HPLC may have arisen not only from the difficulty to identify pico–nano-sized haptophytes in cell counts (which, in addition, can display different morphologies during their life cycle; Thomsen et al. 1994), but also from an overestimation of haptophytes by using Hex-fuco. In this sense, although Hex-fuco has been reported to be the dominant carotenoid in most open oceanic regions (Bidigare and Ondrusek 1996; Gibb et al. 2000), molecular studies have shown that their contribution to the picoeukaryotic community is much lower than expected by pigments (Moon-van der Staay et al. 2000). A possible explanation to this mismatch could be the presence of Hex-fuco in diverse picoeukaryotic lineages still undescribed but detected in molecular studies (Moon-van der Staay et al. 2001). Second, pigment ratios derived from available cultures might certainly be different (especially for the picoplankton) to those of the dominant species in field samples.

The vertical distribution of pigments was particularly interesting regarding the pool of fucoxanthin-related pigments. The highly significant positive correlation of But-fuco and Fuco with depth, and the opposite trend observed for the Hex-fuco contribution, could be interpreted in two ways. First, these trends could reveal a light-induced change in the relative proportion of fucoxanthin derivatives, which has already been reported for Fuco and Hex-fuco in several haptophytes (Schlüter et al. 2000; Stolte et al. 2000), although the photosynthetic benefits underlying these changes are still not well understood. Second, an increase in the importance of chrysophytes/pelagophytes (But-fuco) versus haptophytes with depth has already been reported by several authors (Barlow et al. 1997; Marty et al. 2002), and explained by a nutrient control of their respective vertical distribution.

Furthermore, it would be necessary to implement flow cytometry and molecular techniques (Simon et al. 1994; FISH-TSA, Not et al. 2002; DGGE, Díez et al. 2002) in order to compare pigment distributions, pico–nanoeukaryote abundance and phylogenetic data in oligotrophic environments such as the southern Bay of Biscay in summer. The relative contribution of prokaryotes such as *Synechococcus*-type cyanobacteria should also be contrasted with epifluorescence microscopy or flow cytometry, since zeaxanthin-based estimates could be prone to error due to its detection in other groups such as chlorophytes.

Rings, as well as SWODDIES, show a solid body rotation holding a core of homogeneous water (continental slope current in this study), and as a consequence a distinct semi-isolated assemblage of phytoplankton species evolving from the "source" water mass is expected to occur inside the eddy. The pigment composition observed in the slope current off the northwest coast of Spain was similar to those observed at the SCM of the central region of SWODDY AE6, including some specific marker pigments such as chl c_2–MGDG (14:0/14:0) and gyroxanthin-diester. However, the presence of alloxanthin, DV chl *a* and DV chl *b* in the phytoplankton sample from the slope current shows abundant contributions by cryptophytes and *Prochlorococcus marinus*, which were not apparent in the present study. These changes in the resident plankton community can probably be explained by the effects of the SWODDY on nutrient gradients and light availability, benefiting some algal groups (diatoms, haptophytes) at the expense of previously dominant species (cryptophytes and *P. marinus*) that were better acclimated to oligotrophic conditions on a long-term scale (Garçon et al. 2001).

In conclusion, the results shown herein provide additional evidence of the reliability of HPLC-derived pigments as a tool for the assessment of phytoplankton variability related to a mesoscale eddy structure, and illustrate the advantage inherent in the joint use of chemotaxonomic and traditional methods for the

exploration of phytoplankton composition and distribution at sea. The modification of phytoplankton biomass and composition associated with the presence of the anticyclonic SWODDY AE6 might, in turn, exert a significant effect upon the trophic interactions and organic-matter fluxes of the pelagic ecosystem of the southern Bay of Biscay during the stratified, low-nutrient season.

Acknowledgements This work was supported by the projects CICYT-MAR96-1872-CO3-03AR and PGIDT-CIMA-99/9 (Xunta de Galicia). The authors thank B. Mouriño for helping with the thermohaline data processing.

References

Angel MV, Fasham MJR (1983) Eddies and biological processes. In: Robinson AR (ed) Eddies in marine science. Springer, Berlin Heidelberg New York, pp 492–524

Ansotegui A, Sarobe A, Trigueros JM, Urrutxurtu I, Orive E (2003) Size distribution of algal pigments and phytoplankton assemblages in a coastal estuarine environment: contribution of small eukaryotic algae. J Plankton Res 25:341–355

Barlow RG, Mantoura RFC, Cummings DG, Fileman TW (1997) Pigment chemotaxonomic distributions of phytoplankton during summer in the western Mediterranean. Deep-Sea Res II 44:833–850

Bidigare RR, Ondrusek ME (1996) Spatial and temporal variability of phytoplankton pigment distributions in the central equatorial Pacific Ocean. Deep-Sea Res II 43:809–833

Bjørnland T (1990) Carotenoid structures and lower plant phylogeny. In: Krinsky NI, Mathews-Roth MM, Taylor RF (eds) Carotenoids: chemistry and biology. Plenum, New York

Bjørnland T, Fiksdahl A, Skjetne T, Krane J, Liaaen-Jensen S (2000) Gyroxanthin—the first allenic acetylenic carotenoid. Tetrahedron 56:9047–9056

Daugbjerg N, Hansen G, Larsen J, Moestrup Ø (2000) Phylogeny of some of the major genera of dinoflagellates based on ultrastructure and partial LSU rDNA sequence data, including the erection of three new genera of unarmoured dinoflagellates. Phycologia 39:302–317

Dickson RR, Hughes DG (1981) Satellite evidence of mesoscale eddy activity over the Biscay abyssal plain. Oceanol Acta 4:43–46

Díez B, Pedrós-Alió C, Marsh TL, Massana R (2002) Application of denaturing gradient gel electrophoresis (DGGE) to study the diversity of marine picoeukaryotic assemblages and comparison of DGGE with other molecular techniques. Appl Environ Microb 67:2942–2951

Falkowski PG, Ziemann D, Kolber Z, Bienfang PK (1991) Role of eddy pumping in enhancing primary production in the ocean. Nature 352:55–58

Fryxell GA, Gould Jr E, Balmori ER, Theriot EC (1985) Gulf Stream warm core rings: phytoplankton in two fall rings of different ages. J Plankton Res 7:339–364

Garçon VC, Oschlies A, Doney SC, McGillicudy D, Waniek J (2001) The role of mesoscale variability on plankton dynamics in the North Atlantic. Deep-Sea Res II 48:2199–2226

Garrido JL, Otero J, Maestro MA, Zapata M (2000) The main non-polar chlorophyll *c* from *Emiliania huxleyi* (Prymnesiophyceae) is a chlorophyll c_2–monogalactosyldiacylglyceride ester: a mass spectrometry study. J Phycol 36:497–505

Gibb SW, Barlow RG, Cummings DG, Rees NW, Trees CC, Holligan P, Suggett D (2000) Surface phytoplankton pigment distributions in the Atlantic Ocean: an assessment of basin scale variability between 50°N and 50°S. Prog Oceanogr 45:339–368

Gould WJ, Fryxell GA (1988a) Phytoplankton species composition and abundance in a Gulf Stream warm core ring. I. Changes over a five month period. J Mar Res 46:367–398

Gould WJ, Fryxell GA (1988b) Phytoplankton species composition and abundance in a Gulf Stream warm core ring. II. Distributional patterns. J Mar Res 46:399–428

Hitchcock GL, Langdon C, Smayda TJ (1985) Short-term changes in the biology of a Gulf Stream warm-core ring: phytoplankton biomass and productivity. Limnol Oceanogr 32:919–928

Jeffrey SW, Hallegraeff GM (1980) Studies of phytoplankton species and photosynthetic pigments in a warm core eddy of the East Australian current. I. Summer populations. Mar Ecol Prog Ser 3:285–294

Jeffrey SW, Mantoura RFC, Bjørnland T (1997) Data for the identification of 47 key phytoplankton pigments. In: Jeffrey SW, Mantoura RFC, Wright SW (eds) Phytoplankton pigments in oceanography: guidelines to modern methods. UNESCO, Paris, pp 449–559

Johnsen G, Sakshaug E (1993) Bio-optical characteristics and photoadaptive responses in the toxic and bloom-forming dinoflagellates *Gyrodinium aureoulum*, *Gymnodinium galatheanum*, and two strains of *Prorocentrum minimum*. J Phycol 29:627–642

Lochte K, Pfannkuche O (1987) Cyclonic cold-core eddy in the eastern North Atlantic. II. Nutrients, phytoplankton and bacterioplankton. Mar Ecol Prog Ser 39:153–164

Mackey MD, Mackey DJ, Higgins HW, Wright SW (1996) CHEMTAX—a program for estimating class abundances from chemical markers: application to HPLC measurements of phytoplankton. Mar Ecol Prog Ser 144:265–283

Madelain F, Kerut EG (1978) Evidence of mesoscale eddies in the Northeast-Atlantic from a drifting buoy experiment. Oceanol Acta 1:159–168

Marty J-C, Chiavérini J, Pizay M-D, Avril B (2002) Seasonal and interannual dynamics of nutrients and phytoplankton pigments in the western Mediterranean Sea at the DYFAMED time-series station (1991–1999). Deep-Sea Res II 49:1965–1985

McGillicudy DJ, Robinson AR, Siegel DA, Jannasch HW, Johnson R, Dickey TD, McNeil J, Michaels AF, Knap AH (1998) Influence of mesoscale eddies on new production in the Sargasso Sea. Nature 394:263–266

Millie DF, Schofield O, Kirkpatrick GJ, Johnsen G, Tester OA, Vinyard BT (1997) Detection of harmful algal blooms using photopigments and absorption signature: a case study of the Florida red tide dinoflagellate. Limnol Oceanogr 42:1240–1251

Moon-van der Staay SY, van der Staay GWM, Guillou L, Vaulot D, Claustre H, Medlin LK (2000) Abundance and diversity of prymnesiophytes in the picoplankton community from the equatorial Pacific Ocean inferred from 18S rDNA sequences. Limnol Oceanogr 45:98–109

Moon-van der Staay SY, De Wachter R, Vaulot D (2001) Oceanic 18S rDNA sequences from picoplankton reveal unsuspected eukaryotic diversity. Nature 409:607–610

Not F, Simon N, Biegala I, Vaulot D (2002) Application of fluorescent in situ hybridization coupled with tyramide signal amplification (FISH-TSA) to assess eukaryotic picoplankton composition. Aquat Microb Ecol 28:157–166

Olaizola M, Ziemann DA, Bienfang PK, Walsh WA, Conquest LD (1993) Eddy-induced oscillations of the pycnocline affect the floristic composition and depth distribution of phytoplankton in the subtropical Pacific. Mar Biol 116:533–542

Örnólfsdóttir EB, Pinckney JL, Tester PA (2003) Quantification of the relative abundance of the toxic dinoflagellate *Karenia brevis* (Dinophyta), using unique photopigments. J Phycol 39:449–457

Partensky F, Blanchot J, Vaulot D (1999) Differential distribution of *Prochlorococcus* and *Synechococcus* in oceanic waters: a review. In: Charpy L, Larkum AWD (eds) Marine cyanobacteria. Bull Inst Oceanogr Monaco 19:457–475

Pingree RD, Le Cann B (1989) Celtic and Amorican slope and shelf residual currents. Prog Oceanogr 23:303–338

Pingree RD, Le Cann B (1990) Structure, strength and seasonality of the slope currents in the Bay of Biscay region. J Mar Biol Assoc UK 70:857–885

Pingree RD, Le Cann B (1992a) Three anticyclonic slope water oceanic eddies (SWODDIES) in the southern Bay of Biscay in 1990. Deep-Sea Res 39:1147–1175

Pingree RD, Le Cann B (1992b) Anticyclonic eddy X91 in the southern Bay of Biscay, May 1991 to February 1992. J Geophys Res 97:14353–14367

Porra RJ, Pfündel EE, Engel N (1997) Metabolism and function of photosynthetic pigments. In: Jeffrey SW, Mantoura RFC, Wright SW (eds) Phytoplankton pigments in oceanography: guidelines to modern methods. UNESCO, Paris

Repeta DJ, Bjørnland T (1997) Preparation of carotenoid standards. In: Jeffrey SW, Mantoura RFC, Wright SW (eds) Phytoplankton pigments in oceanography: guidelines to modern methods. UNESCO, Paris, pp 239–260

Richards KJ, Gould WJ (1998) Ocean weather—Eddies in the sea. In: Summerhayes CP, Thorpe SA (eds) Oceanography: an illustrated guide. Manson, Southampton

Rodríguez F, Varela M, Zapata M (2002) Phytoplankton assemblages in the Gerlache and Bransfield Straits (Antarctica Peninsula) determined by light microscopy and CHEMTAX analysis of HPLC pigment data. Deep-Sea Res II 49:723–747

Schlüter L, Møhlenberg F, Havskum H, Larsen S (2000) The use of phytoplankton pigments for identifying and quantifying phytoplankton groups in coastal areas: testing the influence of light and nutrients on pigment/chlorophyll *a* ratios. Mar Ecol Prog Ser 192:49–63

Simon N, Barlow RG, Marie D, Partensky F, Vaulot D (1994) Characterization of oceanic photosynthetic picoeukaryotes by flow cytometry. J Phycol 30:922–935

Smith CL, Richards KJ, Fasham MJ (1996) The impact of mesoscale eddies on plankton dynamics in the upper ocean. Deep-Sea Res 43:1807–1832

Stolte W, Kraay GW, Noordeloos AAM, Riegman R (2000) Genetic and physiological variation in pigment composition of *Emiliania huxleyi* (Prymnesiophyceae) and the potential use of its pigment ratios as a quantitative physiological marker. J Phycol 36:529–539

Teira E, Serret P, Fernández E (2001) Phytoplankton size-structure, particulate and dissolved organic carbon production and oxygen fluxes through microbial communities in the NW Iberian coastal transition zone. Mar Ecol Prog Ser 219:65–83

Thomsen HA, Buck KR, Chavez FP (1994) Haptophytes as components of marine phytoplankton. In: Green JC, Leadbeater BSC (eds) The haptophyte algae. Clarendon, Oxford, pp 187–208

Utermöhl H (1958) Zur Vervollkommnung der quantitative Phytoplankton Methodik. Mitt Int Ver Limnol 9:1–38

Wright SW, Van den Enden RL (2000) Phytoplankton community structure and stocks in the East Australian marginal ice zone (BROKE survey, January–March 1996) determined by CHEMTAX analysis of HPLC pigment signatures. Deep-Sea Res II 47:2363–2400

Zapata M, Garrido JL (1991) Influence of injection conditions in reversed phase high-performance liquid chromatography of chlorophylls and carotenoids. Chromatographia 31:589–594

Zapata M, Rodríguez F, Garrido JL (2000) Separation of chlorophylls and carotenoids from marine phytoplankton: a new HPLC method using a reversed phase C8 column and pyridine-containing mobile phases. Mar Ecol Prog Ser 195:29–45

Zapata M, Edvardsen B, Rodríguez F, Maestro MA, Garrido JL (2001) Chlorophyll c_2 monogalactosyldiacylglyceride ester (chl c_2–MGDG). A novel marker pigment for *Chrysochromulina* species (Prymnesiophyceae). Mar Ecol Prog Ser 219:85–98